



**Bimetallic metal-organic frameworks
 $(\text{H}_3\text{O})_x[\text{Cu}(\text{MF}_6)(\text{pyrazine})_2] \cdot (4-x)\text{H}_2\text{O}$ ($\text{M} = \text{V}^{4+}$, $x = 0$; $\text{M} = \text{Ga}^{3+}$, $x = 1$): co-existence of ordered and disordered
 quantum spins in the V^{4+} system**

Journal:	<i>ChemComm</i>
Manuscript ID	Draft
Article Type:	Communication
Date Submitted by the Author:	n/a
Complete List of Authors:	<p>Manson, Jamie; Eastern Washington University, Chemistry and Biochemistry Schlueter, John A; Argonne National Laboratory, Chemistry and Materials Science Divisions Garrett, Kerry; Eastern Washington University, Chemistry and Biochemistry Goddard, Paul; University of Warrick, Physics Lancaster, Tom; University of Durham, Physics Moeller, Johannes; Oxford University, Clarendon Laboratory and Department of Physics Blundell, Stephen; Oxford University, Clarendon Laboratory and Department of Physics Steele, Andrew; Oxford University, Clarendon Laboratory and Department of Physics Franke-Chaudet, Isabel; Oxford University, Clarendon Laboratory and Department of Physics Pratt, Francis; Rutherford-Appleton Laboratory, ISIS Singleton, John; Los Alamos National Laboratory, National High Magnetic Field Laboratory Bendix, Jesper; University of Copenhagen, Chemistry Lapidus, Saul; Argonne National Laboratory, X-ray Sciences Division, Advanced Photon Source Uhlarz, Marc; Helmholtz-Zentrum Dresden-Rossendorf, Dresden High Magnetic Field Laboratory Ayala-Valenzuela, Oscar; Los Alamos National Laboratory, National High Magnetic Field Laboratory McDonald, Ross; Los Alamos National Laboratories, Gurak, Mary; Los Alamos National Laboratory, National High Magnetic Field Laboratory Baines, Christopher; Paul Scherrer Institut, Laboratory for Muon-Spin Spectroscopy</p>

SCHOLARONE™
Manuscripts



Jamie L. Manson, Ph. D.

Department of Chemistry and Biochemistry
226 Science
Cheney, WA 99004-2440

Cheney • Spokane

July 14, 2016

May Copsey
Executive Editor, *ChemComm*
Thomas Graham House
Science Park, Milton Road
Cambridge CB4 0WF United Kingdom

Dear Ms. Copsey,

We are submitting the manuscript entitled: **“In-situ generation of MF_6^{n-} in bimetallic metal-organic frameworks $(H_3O)_x[Cu(MF_6)(pyrazine)_2] \cdot (4-x)H_2O$ ($M = V^{4+}$, $x = 0$; $M = Ga^{3+}$, $x = 1$): Co-existence of ordered and disordered quantum spins in the V^{4+} system”** by J. L. Manson and co-workers to *Chemical Communications*. All co-authors have read and approve this manuscript which is under exclusive submission to the journal.

Our manuscript describes the *in-situ* generation of novel MF_6^{n-} anions ($M = V^{4+}$, $n = 2$; $M = Ga^{3+}$, $n = 3$) which in turn can be utilized as molecular building blocks. Combining these units with pyrazine (pyz) and Cu^{2+} cations in either HF(aq) or neat H_2O solution leads to coordination polymers of chemical composition $(H_3O)_x[Cu(MF_6)(pyz)_2] \cdot (4-x)H_2O$ ($M = V^{4+}$, $x = 0$; $M = Ga^{3+}$, $x = 1$). Single crystal X-ray diffraction established that each compound forms a tetragonal metal-organic framework composed of 2D $[Cu(pyz)_2]^{2+}$ square lattices linked via bridging MF_6^{n-} . Additional H_2O molecules fill the internal pores and form strong hydrogen bonds with the terminal F's of the MF_6^{n-} moiety. In the case of $M = Ga^{3+}$, one these waters of crystallization is actually H_3O^+ as needed for charge balance. The valence flexibility offered by the MF_6^{n-} species is unique and lends itself to many potential variations of not only the metal but the charge associated with it. In this *Communication*, we retain common Cu-pyz lattices in the two materials but vary the M site and charge – we describe this impact on the magnetic properties.

Two-dimensional antiferromagnetism exhibited by the common Cu-pyz lattice in these materials is easily observed in the $\chi(T)$ data for $M = Ga^{3+}$ but completely obscured in the V^{4+} system due to its fluctuating spin-1/2 moments. The net result is that long-range magnetic order occurs below 3.5 and 2.6 K, respectively, for the V^{4+} and Ga^{3+} compounds. Interestingly, the V^{4+} moments do not undergo LRO down to at least 0.5 K (as shown by both heat capacity and muon-spin relaxation data); pulsed-field magnetization data reveals two effects in the V^{4+} compound; (1) saturation of the Cu^{2+} moments near 28.8 T and (2) hysteresis in the up/down field sweeps at lower fields which is completely absent from the Ga^{3+} data. Thus, the Cu- VF_6 material consists of two magnetic sublattices with only the Cu^{2+} moments making the transition to LRO. This is further corroborated by temperature- and angle-dependent ESR data which are included as supplementary material.

In our view, the synthesis of these two structures suggests that a similar scheme could be used to prepare a large number of other bimetallic derivatives including those of reduced structural dimensionality (i.e., large molecules, chains and/or layers). This particular work showcases one particular derivation and thus we believe it to be worthy of publication in *Chemical Communications*.

This article would be of interest to inorganic/materials chemists, physical chemists, those working in the areas of molecular magnetism and supramolecular chemistry as well as the general readership of the *Journal* and we recommend the following qualified reviewers: Prof. Greg Girolami (Department of Chemistry, University of Illinois at Urbana-Champaign, ggirolam@uiuc.edu), Prof. Kim Dunbar (Department of Chemistry, Texas A & M University, dunbar@mail.chem.tamu.edu), Prof. Mark Meisel (Department of Physics, University of Florida, meisel@phys.ufl.edu), Prof. Dan Talham (Department of Chemistry, University of Florida, talham@chem.ufl.edu), Prof. Mark Turnbull (Department of Chemistry, Clark University, mturnbull@clarku.edu) and Prof. Jan Musfeldt (Department of Chemistry, University of Tennessee, musfeldt@ion.utk.edu).

We appreciate your consideration of this work and look forward to hearing from you soon.

Sincerely,

Jamie L. Manson

Bimetallic metal-organic frameworks $(\text{H}_3\text{O})_x[\text{Cu}(\text{MF}_6)(\text{pyrazine})_2] \cdot (4-x)\text{H}_2\text{O}$ ($M = \text{V}^{4+}$, $x = 0$; $M = \text{Ga}^{3+}$, $x = 1$): co-existence of ordered and disordered quantum spins in the V^{4+} system

Jamie L. Manson^{1*}, John A. Schlueter², Kerry E. Garrett¹, Paul A. Goddard³, Tom Lancaster⁴, Johannes S. Möller³, Stephen J. Blundell³, Andrew J. Steele³, Isabel Franke³, Francis L. Pratt⁵, John Singleton⁶, Jesper Bendix⁷, Saul H. Lapidus², Marc Uhlarz⁸, Oscar Ayala-Valenzuela⁶, Ross D. McDonald⁶, Mary Gurak⁶, Christopher Baines⁹

¹Department of Chemistry and Biochemistry, Eastern Washington University, Cheney, WA 99004, ²Materials Science Division, Argonne National Laboratory, Argonne, IL 60439, ³Clarendon Laboratory, Department of Physics, University of Oxford, Oxford, OX1 3PU UK, ⁴Center for Materials Physics, University of Durham, Durham, DH1 3LE UK, ⁵ISIS Pulsed Muon Facility, Rutherford-Appleton Laboratory, Chilton, Oxfordshire, OX11 0QX UK, ⁶National High Magnetic Field Laboratory, Los Alamos National Laboratory, Los Alamos, NM 87545, ⁷Department of Chemistry, University of Copenhagen, Copenhagen, DK-2100 Denmark, ⁸HochFeld-MagnetLabor, Helmholtz-Zentrum Dresden-Rossendorf, DE-01314 Dresden, Germany, ⁹Paul Scherrer Institut, Laboratory for Muon-Spin Spectroscopy, CH-5232 Villigen PSI, Switzerland.

RECEIVED DATE (automatically inserted by publisher); jmanson@ewu.edu

Low-dimensional metal-organic solids have yielded a plethora of interesting structure types that display a broad range of magnetic behaviors including bistability, slow relaxation of the magnetization, and conventional Néel order.¹ The design of such materials depends on the symmetry, size, reactivity, and stability of the building block(s) used to prepare them. A great advantage of metal-organic systems (relative to metal oxides for example) is their general ease of synthesis and systematic tunability of physical properties by the variation of the metal ion (identity and/or oxidation state) and the organic ligands. For magnetic materials, paramagnetic building blocks are obviously important and the search for new examples with desired properties is an ongoing endeavor.

Discrete perfluoro MF_6^{3-} complexes²⁻⁴ are known for $M = \text{V}^{3+}$, Cr^{3+} , and Fe^{3+} whereas MF_6^{2-} is exceedingly sparse with only one example fortuitously containing VF_6^{2-} .⁵ It would be of great interest to employ these open-shell, valence flexible, complexes as building blocks to synthesize extended structures analogous to Prussian Blues and the like.⁶ It is conceivable that substantially shorter $M\text{-F-M}$ distances could lead to enhanced magnetic couplings relative to the longer $M\text{-C}\equiv\text{N-M}$ despite the lack of significant π -accepting character of F.

Fluoride, with its simultaneous preference for linear bridging and for metal centers in high oxidation states, can direct the self-assembly of extended structures. Here, we report on the bimetallic $[\text{Cu}(\text{VF}_6)(\text{pyz})_2] \cdot 4\text{H}_2\text{O}$ (**1**) and $(\text{H}_3\text{O})[\text{Cu}(\text{GaF}_6)(\text{pyz})_2] \cdot 3\text{H}_2\text{O}$ (**2**) with pyz being pyrazine. The respective VF_6^{2-} and GaF_6^{3-} building blocks were generated *in-situ* from VF_4 and GaF_3 precursors in the presence of aqueous HF.⁷ Their crystal structures consist of 3D metal-organic frameworks (MOF's) composed of 2D $[\text{Cu}(\text{pyz})_2]^{2+}$ square sheets bridged by paramagnetic VF_6^{2-} (**1**) or diamagnetic GaF_6^{3-} (**2**) moieties. Our extensive study of their magnetism reveals that only the Cu^{2+} moments undergo long-range magnetic order (LRO) in both compounds. Thus, we propose that the $S = 1/2$ V^{4+} sites in **1** facilitate an interlayer $\text{Cu}\cdots\text{Cu}$ exchange interaction but themselves remain disordered down to at least 0.5 K.

The structures of **1** and **2** were determined at 100 K using single crystal X-ray diffraction methods.⁸ Both crystallize in the tetragonal space group $P4/nbm$ and have similar unit cell

parameters. The Cu^{2+} ion occupies a 422 symmetry site whereas $\text{V}^{4+}/\text{Ga}^{3+}$ sites reside on inversion centers. Each Cu^{2+} ion is ligated to four N-donor atoms from different pyrazine ligands at distances of 2.050(1) Å (**1**) and 2.045(1) Å (**2**) while the axial Cu-F1 distances are longer at 2.238(2) Å (**1**) and 2.236(1) Å (**2**). The local geometry about the CuN_4F_2 core is very similar for **1**, **2**, and $[\text{Cu}(\text{HF}_2)(\text{pyz})_2]\text{BF}_4$.⁹ In **1**, the V^{4+} center is coordinated to six different F⁻ anions at distances of 1.870(2) (2x) and 1.927(1) Å (4x) for V-F1 and V-F2, respectively. Thus, within experimental error the VF_6^{2-} ion can be described as isotropic; the GaF_6^{3-} anion in **2** behaves similarly.

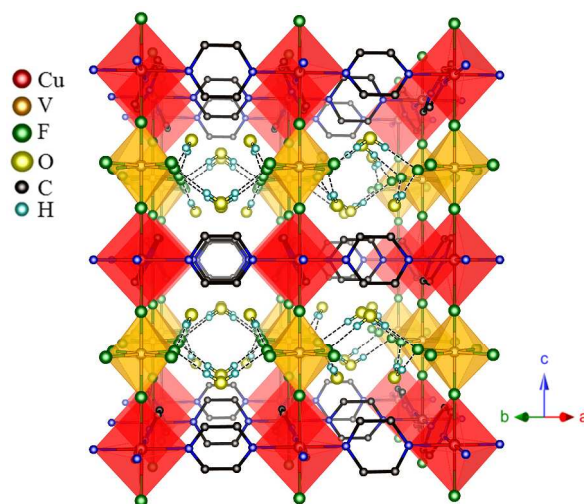


Figure 1. Polyhedral rendition of the metal-organic framework (MOF) for $(\text{H}_3\text{O})_x[\text{Cu}(\text{MF}_6)(\text{pyz})_2] \cdot (4-x)\text{H}_2\text{O}$ (**1**) $M = \text{V}$, $x = 0$; (**2**) $M = \text{Ga}$, $x = 1$. The strong O-H \cdots F hydrogen bonds are delineated by dashed lines. Pyz H-atoms are omitted for clarity.

In **1** and **2**, pyz ligands connect Cu^{2+} centers to form 2D square sheets $[\text{Cu}\cdots\text{Cu} = 6.882(1)$ Å for **1** and $6.868(1)$ for **2**] within the *ab*-plane while bridging $\text{VF}_6^{2-}/\text{GaF}_6^{3-}$ anions link the sheets together $[\text{Cu}\cdots\text{V} = 4.108(1)$ Å for **1**; $\text{Cu}\cdots\text{Ga} = 4.121(1)$ Å for **2**] to afford Cu-F-M-F-Cu chains along the *c*-axis. The result is the

3D polymeric framework depicted in Figure 1. The 4-fold rotational symmetry of the Cu^{2+} site imposes a propeller-like disposition of the pyz ligands, giving a tilt angle of $62.84(6)^\circ$ (**1**) and $63.39(6)^\circ$ (**2**) relative to the CuN_4 equatorial plane. Both angles are greater/less than the corresponding angles of $59.4(2)/81.4(1)^\circ$ found in $[\text{Cu}(\text{HF}_2)(\text{pyz})_2]\text{BF}_4$ and its SbF_6^- analog.^{9,10} The MF_4 plane (that contains F2's) within the MF_6^{n-} core is rotated about the c -axis by 45° relative to CuN_4 thus, all MF_6^{n-} octahedra along the c -direction share identical orientations. Waters of crystallization occupy each pore and form hydrogen bonds with terminal F atoms from MF_6^{n-} octahedra [(**1**): $\text{H1A-F2} = 1.86(1) \text{ \AA}$, $\text{O1-H1A-F2} = 176(2)^\circ$; (**2**): $\text{H1-F1} = 1.85(1) \text{ \AA}$, $\text{O1-H1-F1} = 178(2)^\circ$]. For **2**, one out of every four H_2O 's is a charge-compensating H_3O^+ cation, and because of the 4-fold symmetry of those sites, the proton is positionally disordered. Electron-density difference maps support this conclusion.

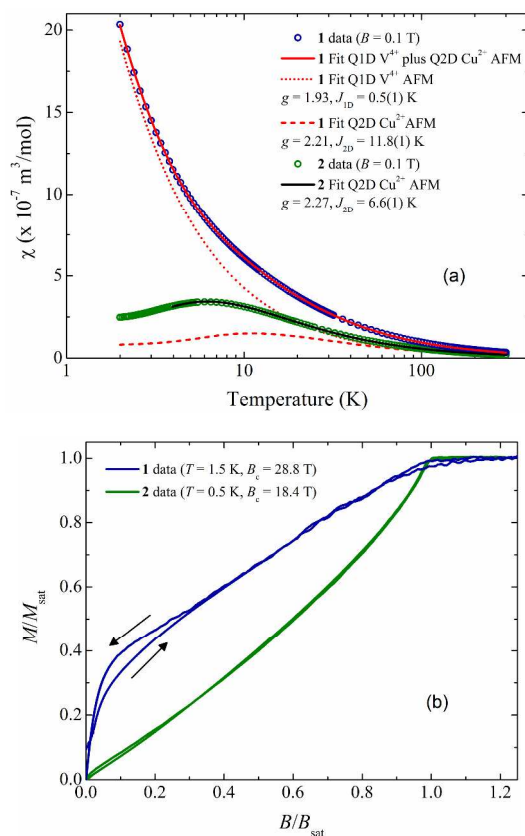


Figure 2. (a) Magnetic susceptibility data (open symbols) for **1** and **2**. Solid lines represent theoretical fits as described in the text. (b) Pulsed-field magnetization data for **1** and **2** at low temperatures.

The magnetic susceptibility $\chi(T)$ obtained for polycrystalline samples of **1** and **2** between 2 and 300 K are shown collectively in Figure 2a. At first glance, **1** appears to be paramagnetic without any anomalies that would have indicated a magnetic phase transition whereas **2** displays a broad maximum at 6 K, a feature typical of other quasi-2D coordination polymers including $\text{Cu}(\text{ClO}_4)_2(\text{pyz})_2$ ¹¹ and $[\text{Cu}(\text{HF}_2)(\text{pyz})_2]\text{X}$ ($\text{X} = \text{BF}_4^-$, PF_6^- , SbF_6^- , TaF_6^-) that show short-range spin correlations.⁹⁻¹³ The lack of a maximum in $\chi(T)$ for **1** suggests that the additional fluctuating (i.e., paramagnetic) V^{4+} spin likely masks this feature. Being that Ga^{3+} in **2** is a closed-shell cation, the expected magnetic lattice is 2D and should produce the observed broad maximum in $\chi(T)$.

The crystal structures of **1** and **2** contain common 2D $[\text{Cu}(\text{pyz})_2]^{2+}$ square lattices, and as such, the primary exchange is

governed by Cu-pyz-Cu pathways (J_{2D}). Electron-spin resonance experiments (see SI) confirm that the Cu^{2+} magnetic $d_{x^2-y^2}$ orbital lies in the 2D CuN_4 plane for both **1** and **2**. Considering an additional (albeit weak) exchange interaction along V-F-Cu-F-V (J_{1D}) in **1**, the $\chi(T)$ data may be described by an antiferromagnetic (AFM) Heisenberg $S = 1/2$ model ($\hat{H} = J\sum_i \vec{S}_i \cdot \vec{S}_{i+1}$) based on the sum of two components; a 2D quadratic lattice¹⁴ and a 1D chain.¹⁵ For **2**, only the quadratic model was required. In Figure 2a, the results of the least-squares fit give excellent reproducibility with the data for the following parameters; $g_{\text{Cu}} = 2.21(1)$, $g_{\text{V}} = 1.93(1)$, $J_{2D} = 11.8(1) \text{ K}$, and $J_{1D} = 0.5(1) \text{ K}$ for **1** and $g_{\text{Cu}} = 2.27(1)$ and $J_{2D} = 6.6(1) \text{ K}$ for **2**. The fitted Landé g -factors are average values and agree with the ESR-determined values.

Pulsed-field magnetization¹⁶ data for **1** and **2** acquired up to 40 T and at $T = 0.5 \text{ K}$ are shown in Figure 2b. The main difference exhibited by the two compounds is the low-field region below $\sim 10 \text{ T}$ where **1** shows hysteresis between up- and down-field sweeps which is attributed to fluctuating V^{4+} moments. Above 10 T, the magnetization rises in a concave fashion which is indicative of low-dimensional spin interactions.¹⁶ In contrast, **2** shows only a concave rise in the magnetization with a critical field (B_c) of 18.4 T (as determined by the midpoint of the gradient in dM/dB) which is substantially less than the 28.8 T critical field found in **1**. We can use these critical fields to independently deduce J_{2D} based on the simple relationship, $J_{2D} \approx g_{\text{Cu}}B_c/6.03 \text{ T}$,¹⁶ which gives 10.6(1) K ($g_{\text{Cu}} = 2.21$) and 6.8(1) K ($g_{\text{Cu}} = 2.27$) for **1** and **2**, respectively, of which the latter J_{2D} is in line with the value obtained from the fit of $\chi(T)$. We attribute the slight discrepancy between calculated and fitted J_{2D} 's for **1** as being due to the gradual approach to saturation resulting in a broadened transition.

The Cu-pyz-Cu magnetic interaction for **1** and **2** can be rationalized by superexchange via the σ -bond network containing adjacent Cu magnetic $d_{x^2-y^2}$ orbitals and lone-pair orbitals located on N-atoms. The weak interaction mediated along V-F-Cu-F-V is not surprising in that the spin-paired d_z^2 orbital (of Cu) overlaps the p_z orbital of F ligands. Because F has no practical π -acceptor character, any interaction along this pathway is likely facilitated by mixing of the Cu $d_{x^2-y^2}$ and d_z^2 orbitals. In addition, the single V^{4+} electron resides in a π -type orbital (i.e., d_{xy} , d_{xz} , or d_{yz}). Its overlap with $d_{x^2-y^2}(\text{Cu})$, although not zero by symmetry due to the relative orientations of the CuN_4F_2 and VF_6^{2-} octahedra, is predicted to be quite small.

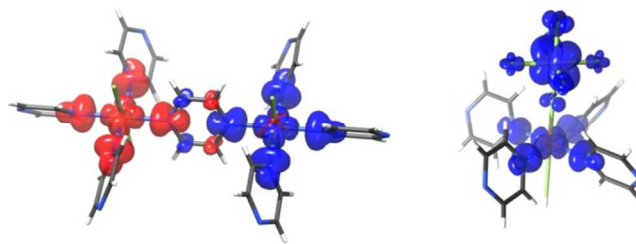


Figure 3. DFT computed spin density distributions for the *trans, trans*- $[(\text{pyz})_3\text{CuF}_2(\mu\text{-pyz})\text{CuF}_2(\text{py})_3]$ (left) and *trans*- $[(\text{HF})\text{Cu}(\text{py})_4(\mu\text{-F})\text{VF}_5]$ (right). Isosurface values are ± 0.00087 and $\pm 0.002 \text{ 1/\AA}^3$, respectively.

Broken symmetry Density-Functional Theoretical (DFT) calculations¹⁷ were undertaken for **1** in order to corroborate this picture. Calculations were performed on dinuclear fragments of the experimental structure namely, *trans, trans*- $[(\text{pyz})_3\text{CuF}_2(\mu\text{-pyz})\text{CuF}_2(\text{py})_3]$ and *trans*- $[(\text{HF})\text{Cu}(\text{py})_4(\mu\text{-F})\text{VF}_5]$. In the latter case a proton was added to the terminal fluoride on copper in an optimized position with $\text{F}_{\text{Cu}}\text{-H}$ of 1.18 \AA in order for both fragments to have the same charge. The computed spin density

distributions for the two fragments are shown in Figure 3. The exchange coupling constants were calculated to be AFM (12.6 K) and FM (-0.29 K), supporting the experimental picture of a 2D magnetic structure with only very weak interactions along the V-F-Cu-F-V chains. Attempts to constrain $J > 0$ in the fit of $\chi(T)$ leads to g -factors different from those obtained by ESR. In either case $|J_{\text{D}}|$ is consistently small and a spin polarization mechanism seemingly fails to explain the experimental result for Cu-F-V.

The presence of LRO in **1** and **2** was confirmed by muon-spin relaxation (μSR) measurements carried out at the STFC ISIS Facility, Rutherford-Appleton Laboratory (UK) using a sorption cryostat on the MuSR beamline and at the Swiss Muon Source, Paul Scherrer Institut (Switzerland) using the LTF instrument.

In data measured on **1** we observe oscillations in the muon polarization below 3.5 K at a single frequency. These oscillations reflect the coherent precession of muon spins about a local quasistatic B -field implying that the system is in a state of LRO. The precession frequency ν is plotted against T in Figure 4. The frequency ν may be taken as an effective order parameter for the system, and is fitted to the phenomenological function $\nu(T) = \nu(0)(1 - (T/T_N)^{\alpha})^{\beta}$. We obtain a fitted value for the critical temperature of $T_N = 3.5(2)$ K and an exponent $\beta = 0.33(3)$, the latter suggesting that fluctuations in this system have a three-dimensional character. The observed behavior of **1** is similar to other $S=1/2$ Cu^{2+} molecular magnets studied previously¹⁸ in both transition temperature and magnitude of internal field at the muon site. However, the oscillations observed for this system are significantly more damped than found in previous cases, likely caused by spatial or temporal fluctuations of magnetic moments on the V^{4+} ions. Data measured above 3.5 K show slow, heavily damped oscillations attributable to dipole-dipole interactions between muons and ^{19}F nuclei as observed previously in other fluorine-containing molecule-based magnets.¹⁹

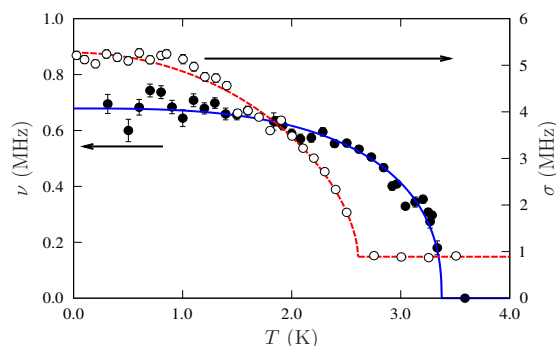


Figure 4. Evolution of the muon spin precession frequency ν for **1** (filled circles) and the Gaussian relaxation rate σ for **2** (unfilled circles). The blue line denotes the fit described in the text; the red line is a guide to the eye.

In the data measured on **2** no well-resolved oscillations exist at any measured temperature down to 0.025 K, indicating a broader distribution of magnetic fields in **2** compared to **1**. However, there is a distinct change in shape of the muon spectra below 2.6 K involving a sizeable increase in the Gaussian relaxation rate σ . This relaxation rate represents the width of the local field distribution experienced by the muon ensemble and is expected to scale with the magnitude of the average local field. The evolution of σ with temperature is also shown in Figure 4 and closely resembles the expected order parameter behavior, decreasing as 2.6(1) K is approached from below. Taken together with the

discontinuous decrease in the non-relaxing muon polarization above T_N (which often accompanies a magnetic ordering transition),¹⁸ we conclude that **2** undergoes a transition to a state of LRO below $T_N = 2.6(1)$ K.

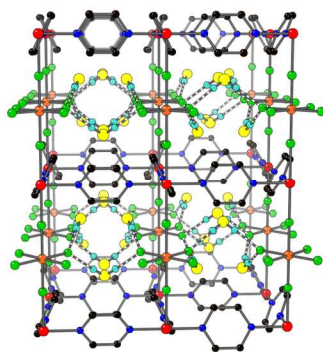
ACKNOWLEDGMENT. Work at EWU was supported by the NSF under grant no. DMR-1306158. Research supported by UChicago Argonne, LLC, operator of Argonne National Laboratory ("Argonne"). Argonne, a U. S. Department of Energy (DoE) Office of Science Laboratory, is operated under contract no. DE-AC02-06CH11357. This work was also supported by the EPSRC, UK and EuroMagNET under EU contract No. 228043. We are grateful to the STFC ISIS Facility and to the Swiss Muon Source for the provision of beamtime. Work at the NHMFL was conducted under the auspices of the NSF, the DoE BES program "Science in 100 T" and the State of Florida.

SUPPORTING INFORMATION

CIF's for **1** and **2** at 100 K, CCDC XXXXXX-XXXXXX, contains the supplementary crystallographic data for this paper. These data can be obtained free of charge from the Cambridge Crystallographic Data Centre via www.ccdc.cam.ac.uk/data_request/cif. Thermal ellipsoid plots containing atom numbering schemes and ESR data. This information is available via the Internet at <http://pubs.acs.org>.

REFERENCES

- [1] Magnetism: Molecules to Materials, Vols. 1-5; Miller, J. S.; Drillon, M., Eds.; Wiley-VCH: Weinheim, 2002-2004, and references therein.
- [2] Fourquet, J. L.; Plet, F.; Calage, Y.; de Pape, R.; *J. Solid State Chem.* **1987**, *69*, 76.
- [3] Ali, A. B.; Dang, M. T.; Greneche, J.-M.; Hemon-Ribaud, A.; Leblanc, M.; Maisonneuve, V. *J. Solid State Chem.* **2007**, *180*, 1911.
- [4] Aldous, D. W.; Stephens, N. F.; Lightfoot, P. *Dalton Trans.* **2007**, 2271.
- [5] Mahenthirarajah, T.; Li, Y.; Lightfoot, P. *Inorg. Chem.* **2008**, *47*, 9097.
- [6] for a review, see: Herrera, J. M.; Bachschmidt, A.; Villain, F.; Bleuzen, A.; Marvaud, V.; Wernsdorfer, W.; Verdager, M. *Phil. Trans. R. Soc. A* **2008**, *366*, 127.
- [7] Stoichiometric amounts of CuF_2 , VF_4 and pyrazine were dissolved together in 48% HF(aq) to give a blue-green solution. Upon slow evaporation of the solvent overnight, X-ray quality blue prisms of **1** were formed in high yield. Blue plates of **2** were obtained by the reaction of CuF_2 , GaF_3 , NH_4HF_2 and pyrazine in H_2O with slow evaporation of the solvent.
- [8] Crystallographic data for **1**: $\text{C}_8\text{H}_{16}\text{N}_4\text{F}_6\text{O}_4\text{VCu}$, $M = 460.73$, tetragonal, space group $P4/nbm$, $a = b = 9.7325(2)$, $c = 8.2154(1)$ Å, $U = 778.18(2)$ Å³, $T = 100$ K, $Z = 2$, $\mu(\text{MoK}\alpha) = 2.056$ mm⁻¹, 9707 reflections measured, 626 unique ($R_{\text{int}} = 0.0195$) which were used in all calculations. The final agreement factors were $R_1 = 0.0220$, $wR_2 = 0.0660$, $\text{GoF} = 0.816$. For **2**: $\text{C}_8\text{H}_{16}\text{N}_4\text{F}_6\text{O}_4\text{GaCu}$, $M = 479.50$, tetragonal, space group $P4/nbm$, $a = b = 9.7134(2)$, $c = 8.2415(1)$ Å, $U = 777.59(2)$ Å³, $T = 100$ K, $Z = 2$, $\mu(\text{MoK}\alpha) = 3.189$ mm⁻¹, 9957 reflections measured, 761 unique ($R_{\text{int}} = 0.0172$) which were used in all calculations. The final agreement factors were $R_1 = 0.0203$, $wR_2 = 0.0558$, $\text{GoF} = 1.135$.
- [9] Manson, J. L.; Conner, M. M.; Schlueter, J. A.; Lancaster, T.; Blundell, S. J.; Brooks, M. L.; Pratt, F. L.; Papageorgiou, T.; Bianchi, A. D.; Wosnitza, J.; Whangbo, M.-H. *Chem. Commun.* **2006**, 4894.
- [10] Manson, J. L.; Schlueter, J. A.; Funk, K. A.; Southerland, H. I.; Twamley, B.; Lancaster, T.; Blundell, S. J.; Baker, P. J.; Pratt, F. L.; Singleton, J.; McDonald, R. D.; Goddard, P. A.; Sengupta, P.; Batista, C. D.; Ding, L.; Lee, C.; Whangbo, M.-H.; Franke, I.; Cox, S.; Baines, C.; Trial, D. *J. Amer. Chem. Soc.* **2009**, *131*, 6733.
- [11] Woodward, F. M.; Gibson, P. J.; Jameson, G. B.; Landee, C. P.; Turnbull, M. M.; Willett, R. D. *Inorg. Chem.* **2007**, *46*, 4256.
- [12] Čizmar, E.; Zvyagin, S. A.; Beyer, R.; Uhlarz, M.; Ozerov, M.; Skourski, Y.; Manson, J. L.; Schlueter, J. A.; Wosnitza, J. *Phys. Rev. B* **2010**, *81*, 064422.
- [13] Manson, J. L.; Schlueter, J. A.; McDonald, R. D.; Singleton, J. *J. Low Temp. Phys.* **2010**, *159*, 15.
- [14] Woodward, F. M.; Albrecht, A. S.; Wynn, C. M.; Landee, C. P.; Turnbull, M. M. *Phys. Rev. B* **2002**, *65*, 144412.
- [15] Klümper, A.; Johnston, D. C. *Phys. Rev. Lett.* **2000**, *84*, 4701.
- [16] Goddard, P. A.; Singleton, J.; Sengupta, P.; McDonald, R. D.; Lancaster, T.; Blundell, S. J.; Pratt, F. L.; Cox, S.; Harrison, N.; Manson, J. L.; Southerland, H. I.; Schlueter, J. A. *New J. Phys.* **2008**, *10*, 083025.
- [17] The computational approach has been detailed previously: Manson, J. L. *et al. Inorg. Chem.* **2011**, *50*, 5990 and references therein.
- [18] Steele, A. J.; Lancaster, T.; Blundell, S. J.; Baker, P. J.; Pratt, F. L.; Baines, C.; Conner, M. M.; Southerland, H. I.; Manson, J. L.; Schlueter, J. A. *Phys. Rev. B* **2011**, *84*, 064412.
- [19] Lancaster, T.; Blundell, S. J.; Baker, P. J.; Brooks, M. L.; Hayes, W.; Pratt, F. L.; Manson, J. L.; Conner, M. M.; Schlueter, J. A. *Phys. Rev. Lett.* **2007**, *99*, 267601.



Independent *in-situ* generation of VF_6^{2-} and GaF_6^{3-} anions in aqueous solution leads to the self-assembly of novel bimetallic metal-organic frameworks $(\text{H}_3\text{O})_x[\text{Cu}(\text{MF}_6)(\text{pyz})_2] \cdot (4-x)\text{H}_2\text{O}$ [**1**] $M = \text{V}^{4+}$, $x = 0$; [**2**] $M = \text{Ga}^{3+}$, $x = 1$; pyz = pyrazine). Long-range magnetic ordering of the Cu^{2+} sublattice occurs below 3.5 and 2.6 K for **1** and **2**, respectively. However in **1** we also find evidence for fluctuating V^{4+} moments which remain disordered down to at least 0.5 K.

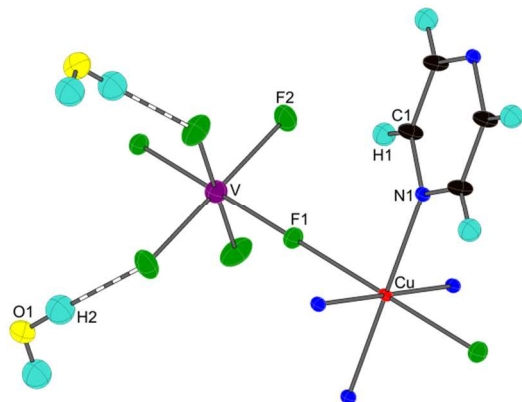
Supplementary information:

Bimetallic metal-organic frameworks $(\text{H}_3\text{O})_x[\text{Cu}(\text{MF}_6)(\text{pyrazine})_2] \cdot (4-x)\text{H}_2\text{O}$ ($M = \text{V}^{4+}$, $x = 0$; $M = \text{Ga}^{3+}$, $x = 1$): Co-existence of ordered and disordered quantum spins in the V^{4+} system

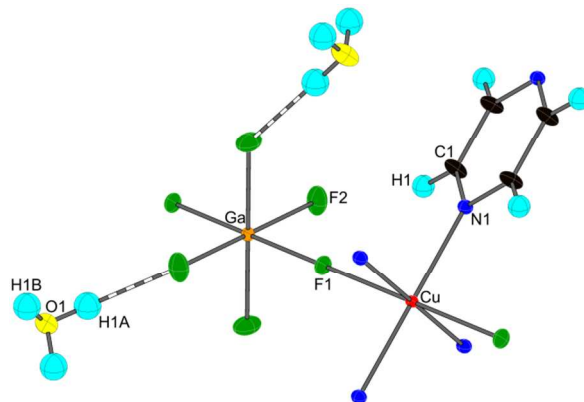
Jamie L. Manson^{1*}, John A. Schlueter², Kerry E. Garrett¹, Paul A. Goddard³, Tom Lancaster⁴, Johannes S. Möller³, Stephen J. Blundell³, Andrew J. Steele³, Isabel Franke³, Francis L. Pratt⁵, John Singleton⁶, Jesper Bendix⁷, Saul H. Lapidus², Marc Uhlarz⁸, Oscar Ayala-Valenzuela⁶, Ross D. McDonald⁶, Mary Gurak⁶, Christopher Baines⁹

¹Department of Chemistry and Biochemistry, Eastern Washington University, Cheney, WA 99004, ²Materials Science Division, Argonne National Laboratory, Argonne, IL 60439, ³Clarendon Laboratory, Department of Physics, University of Oxford, Oxford, OX1 3PU UK, ⁴Center for Materials Physics, University of Durham, Durham, DH1 3LE UK, ⁵ISIS Pulsed Muon Facility, Rutherford-Appleton Laboratory, Chilton, Oxfordshire, OX11 0QX UK, ⁶National High Magnetic Field Laboratory, Los Alamos National Laboratory, Los Alamos, NM 87545, ⁷Department of Chemistry, University of Copenhagen, Copenhagen, DK-2100 Denmark, ⁸HochFeld-MagnetLabor, Helmholtz-Zentrum Dresden-Rossendorf, DE-01314 Dresden, Germany, ⁹Paul Scherrer Institut, Laboratory for Muon-Spin Spectroscopy, CH-5232 Villigen PSI, Switzerland.

Thermal ellipsoid plots (35% probability factors) and atom numbering schemes:

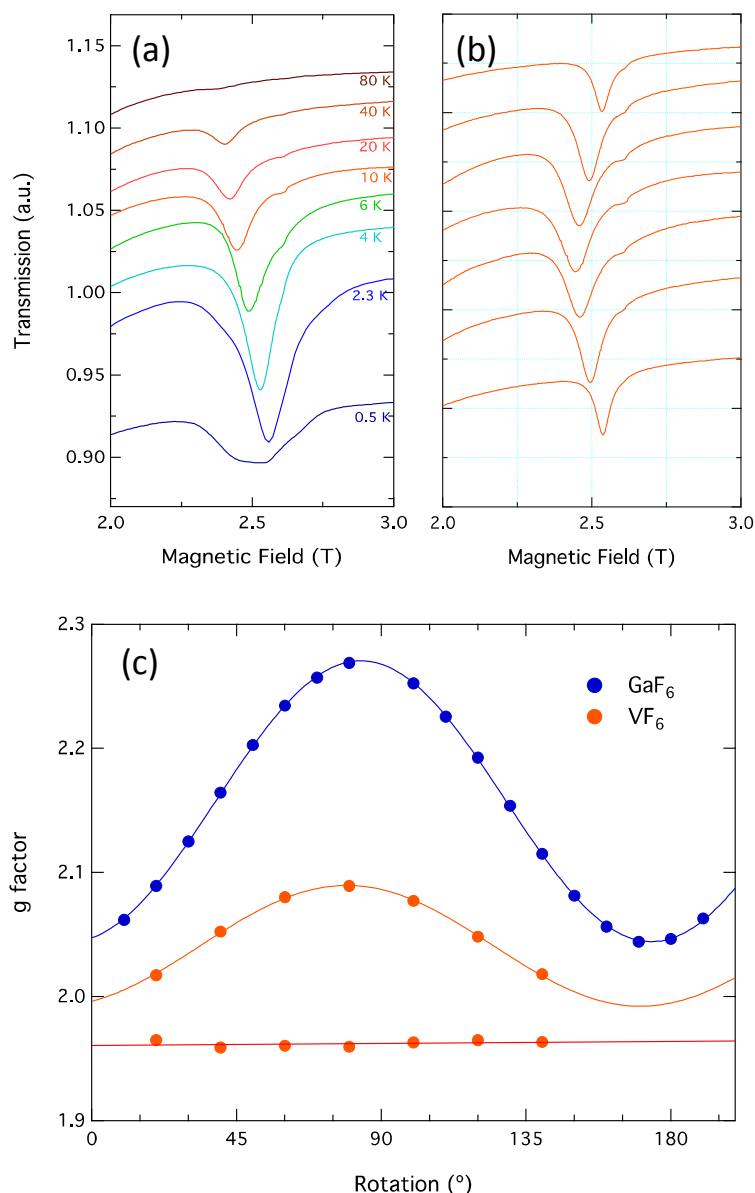


$[\text{Cu}(\text{VF}_6)(\text{pyz})_2] \cdot 4\text{H}_2\text{O}$



$(\text{H}_3\text{O})[\text{Cu}(\text{GaF}_6)(\text{pyz})_2] \cdot 3\text{H}_2\text{O}$

Electron paramagnetic resonance spectra:



(a) Temperature-dependence of the EPR spectrum of $[\text{Cu}(\text{VF}_6)(\text{pyz})_2] \cdot 4\text{H}_2\text{O}$ measured at 71.4 GHz for field aligned perpendicular to the c -axis. At high temperature, two absorption lines are visible corresponding to $g = 2.08$ At 2.45 T and $g = 1.96$ at 2.60 T. As antiferromagnetism is approached below 10 K, the stronger line broadens and shifts to higher fields obscuring the weaker line.

(b) Angular-dependence (in 20° increments about field parallel to the c -axis) of the EPR spectrum for $[\text{Cu}(\text{VF}_6)(\text{pyz})_2] \cdot 4\text{H}_2\text{O}$ measured at 10 K. At this temperature the spectrum is indicative of the paramagnetic g -factor anisotropy, with minimal contribution from spin-anisotropy in the antiferromagnetic exchange interaction.

(c) Comparison of the g -factor anisotropy of $(\text{H}_3\text{O})[\text{Cu}(\text{GaF}_6)(\text{pyz})_2] \cdot 3\text{H}_2\text{O}$ and $[\text{Cu}(\text{VF}_6)(\text{pyz})_2] \cdot 4\text{H}_2\text{O}$ measured at 71.4 GHz and 10 K in the paramagnetic state. The g -anisotropy (2.04-2.27) of $(\text{H}_3\text{O})[\text{Cu}(\text{GaF}_6)(\text{pyz})_2] \cdot 3\text{H}_2\text{O}$ is typical of $3d^9 \text{Cu}^{2+}$ in an octahedral crystal field environment. The isotropic g -factor of 1.96 in $[\text{Cu}(\text{VF}_6)(\text{pyz})_2] \cdot 4\text{H}_2\text{O}$ likely originates from the V^{4+} and mildly anisotropic g -factor (1.99- 2.08) from Cu^{2+} , albeit in a more symmetric crystal field than the Ga^{3+} analogue.